

LETTER • OPEN ACCESS

## On the signature of the cirrus twilight zone

To cite this article: Uri Wollner *et al* 2014 *Environ. Res. Lett.* **9** 094010

View the [article online](#) for updates and enhancements.

You may also like

- [Mixed-phase regime cloud thinning could help restore sea ice](#)  
D Villanueva, A Possner, D Neubauer et al.
- [Modification of cirrus clouds to reduce global warming](#)  
David L Mitchell and William Finnegan
- [Climate impact of aircraft-induced cirrus assessed from satellite observations before and during COVID-19](#)  
Johannes Quaas, Edward Gryspeerdt, Robert Vautard et al.



**The Breath Biopsy® Guide**  
Fourth edition

DOWNLOAD THE FREE E-BOOK

BREATH BIOPSY

OWLSTONE MEDICAL

# On the signature of the cirrus twilight zone

Uri Wollner<sup>1</sup>, Ilan Koren<sup>1</sup>, Orit Altaratz<sup>1</sup> and Lorraine A Remer<sup>2</sup>

<sup>1</sup>Department of Earth and Planetary Sciences, The Weizmann Institute of Science, Rehovot, Israel

<sup>2</sup>Joint Center for Earth Systems Technology, University of Maryland Baltimore County, Baltimore, MD, USA

E-mail: [Ilan.Koren@weizmann.ac.il](mailto:Ilan.Koren@weizmann.ac.il)


Received 22 May 2014, revised 18 August 2014

Accepted for publication 18 August 2014

Published 24 September 2014

## Abstract

Cirrus clouds are known to play a key role in the climate system, but their overall effect on Earth's radiation budget is not yet fully quantified. The uncertainties are, in part, due to ambiguities in cirrus extent or coverage. Here we show that despite careful filtering of cloudy pixels, cirrus clouds have a clear statistical signature. This signature can be estimated by the proximity to detectable cirrus clouds. Such a residual signature can affect retrievals that rely on a cloud-free atmosphere, such as aerosol optical depth (AOD) or sea surface temperature. Analyzing MODIS raw-data and products, we show a clear increase in the reflectance when approaching detectable cirrus clouds. We estimated a mean increase in AOD of  $0.03 \pm 0.01$  and a decrease in the Angstrom-exponent of  $-0.22 \pm 0.20$  in the first kilometer around detectable cirrus. The effect decays tenfold at a typical distance of  $5.5 \pm 1.8$  km. Such trends confirm the contribution of large particles that are likely to be ice crystals to the so-called cloud-free atmosphere near detectable cirrus clouds.

 Online supplementary data available from [stacks.iop.org/ERL/9/094010/mmedia](http://stacks.iop.org/ERL/9/094010/mmedia)


Keywords: twilight, cirrus, aerosols

## 1. Introduction

High-level cirrus clouds are comprised of optically thin ice crystals (Heymsfield and Miloshevich 2003) distributed globally at the top of the troposphere and within the tropopause. Their estimated mean global coverage is 20–30% (Rossow and Schiffer 1999, Wylie *et al* 2005), and their greatest coverage is in the tropics (up to 40%, Sassen and Wang 2008), coinciding with anvil clouds of deep convective systems. Cirrus clouds are abundant at mid-latitudes as well, and their formation mechanisms are associated with jet streams, warm fronts and deep convective systems (anvils). The term 'cirrus' is used herein as a general term describing cirrocumulus (CC), cirrostratus (CS) and cirrus (Ci) clouds. Unlike aerosols that are relatively fine and active mostly in the shortwave, cirrus clouds affect the Earth's radiation budget by reflecting part of the incoming solar radiation back

to space and trapping part of the outgoing terrestrial energy within the system (Koren *et al* 2010b). Nonetheless, their net regional and global effects remain uncertain, partly due to uncertainties in cirrus clouds' spatial extent, and variations in the shapes and sizes of their ice crystals (e.g. Heymsfield and Miloshevich 2003, Field *et al* 2007, 2008, Baran 2012), which in turn affect their directional scattering properties (e.g. Macke *et al* 1996, Edwards *et al* 2007, Baran 2012).

Cirrus cloud detection from space poses a significant challenge, as some cirrus clouds are optically thin (Dessler and Yang 2003). Their low optical depth often makes them undetectable in the visible solar channels (Sassen *et al* 1989, Roskovensky and Liou 2003). However, even optically thin cirrus clouds will affect Earth's radiation balance in the shortwave (Khvorostyanov and Sassen 2002, Futyan *et al* 2005, Dupont and Haeffelin 2008, Barja and Antuña 2011) and, more importantly, in the thermal infrared (e.g. Futyan *et al* 2005, Lee *et al* 2006, Dupont and Haeffelin 2008) regions, and thus cannot be ignored even if they cannot be detected. Lee *et al* (2010) estimated the global annual mean radiative effect of high thin clouds to be  $0.49 \text{ W m}^{-2}$  heating at the top of the atmosphere.

 Content from this work may be used under the terms of the Creative Commons Attribution 3.0 licence. Any further distribution of this work must maintain attribution to the author(s) and the title of the work, journal citation and DOI.

Similar to cirrus clouds, aerosols suspended in the atmosphere often have a weak optical signature relative to the background and instrument noise (Tanré *et al* 1996, 1997, Kahn *et al* 2005). The inversion of spaceborne measurements becomes especially challenging when one attempts to retrieve aerosol properties near clouds (Zhang *et al* 2005, Kaufman *et al* 2005, Koren *et al* 2010a). Previous studies examining aerosol properties near convective clouds found several effects that enhance the apparent aerosol optical depth (AOD). The first is cloud contamination, which consists of undetectably small or optically thin clouds (Koren *et al* 2007, 2009) that are falsely retrieved as aerosols. The second is aerosol humidification: swelling of aerosols in a humid environment (Koren *et al* 2007, Charlson *et al* 2007, Twohy *et al* 2009) and the last is the 3D cloud effect when clouds serve as a source of photons that escape from the sides of the clouds and into the path of a cloud-free retrieval (Marshak *et al* 2006, Wen *et al* 2007).

In most cases, it is easier to separate aerosols from convective clouds than from cirrus clouds due to the former's inherent spatial variability, while both cirrus and aerosols are often spatially smooth (Martins *et al* 2002, Gao *et al* 2002b). Previous cloud-contamination studies of thin cirrus clouds ('cirrus contamination') have shown different detection efficiencies for different space borne sensors. Lidar can detect cirrus clouds with an optical depth of  $10^{-4}$  (for visible wavelengths, Immler and Schrems 2002), whereas passive sensors require the much higher optical depth of  $\sim 0.1$  (Sassen and Wang 2008). Huang *et al* (2011, 2013) used a combination of ground measurements (AERONET, MPLNET) and satellite data (MODIS, CALIPSO) to show possible biases in aerosol optical-thickness retrievals by passive satellite sensors due to contamination by thin cirrus clouds. The operational algorithm for cirrus detection as part of the MODIS cloud product is defined as the MODIS Cirrus Flag (MCF) (Ackerman *et al* 1998, King *et al* 2003). The MCF detects cirrus clouds using the MODIS  $1.38\ \mu\text{m}$  channel in conjunction with a visible channel (Gao *et al* 2002a). It quantifies the cirrus reflectance in the visible spectral range, which is proportional to the cirrus optical thickness. Huang *et al* (2013) analyzed data from the passive MODIS and the active CALIPSO instruments with respect to the effectiveness and robustness of eight MODIS-derived cirrus-screening parameters. They showed that the successful detection rate of thin cirrus was in the range of 65–67%, and the false detection rate (defined as detected cirrus by the MODIS algorithm but not by CALIPSO) was in the range of 35–54% (these ranges do not include the lowest evaluated thin cirrus detection rate of the cloud phase infrared approach). The MCF algorithm yielded a relatively high cirrus detection success-rate of 67% and its false detection rate was 35% over ocean regions.

The MODIS aerosol product does not use the MCF. Instead it identifies cirrus clouds using a procedure that depends on the  $1.38\ \mu\text{m}$  channel through both spectral (Gao *et al* 2002b) and spatial variability tests (Martins *et al* 2002, Remer *et al* 2005). AOD is retrieved for pixels that passed the tests for being free of cloud contamination, cloud shadows, or other unusual conditions. Despite extensive efforts in cirrus

and other clouds detection, the MODIS AOD has been characterized as artificially enhanced by cirrus contamination by 0.01–0.02 over oceans on a global annual basis (Kaufman *et al* 2005). The new collection-6 MODIS aerosol products presents improved cirrus detection algorithm (Levy *et al* 2013). In this study we tested data from both collection 5 and 6.

If both cirrus clouds and aerosol appear as thin veils of enhanced reflectance to a satellite sensor, does it matter whether that thin veil is characterized as cirrus or aerosol? Yes, it does. First, most cirrus clouds can be considered natural phenomena whereas a significant proportion of aerosol loading is anthropogenic. In addition, there are important differences in their radiative effects. Because aerosol particles are generally much smaller and more spherical than cirrus ice crystals, their optical properties differ significantly. For the same visible reflectance measured by satellite, the aerosol and cirrus optical thicknesses can differ by an order of magnitude (compare lookup table curves of Meyer *et al* 2004 with figure 11 in Levy *et al* 2005). Moreover, due to differences in size as well as in their absorption spectra, their interactions with long-wave radiation are completely different. This introduces significantly different perturbations in the Earth's energy balance if the full solar and terrestrial spectra are considered (Lee *et al* 2006). We therefore need to identify thin cirrus clouds by satellite measurements and separate them from aerosol, even when the former are not detectable by deterministic means.

The distance from the nearest detectable cloud has been suggested as a statistical measure for the likelihood of having a contribution from undetectable ones (Koren *et al* 2007). Bar-Or *et al* (2011) showed that the effect in the satellite-measured reflectance can be traced as far as 30 km from the nearest cloud over the Atlantic Ocean. Here we use the same approach, looking on the so-called 'cloud free' atmosphere in the vicinity of cirrus clouds. We hypothesize that similarly to what was shown for other cloud types, there is no sharp threshold (in reflectance or in any other parameter) that can assure an atmosphere free of cirrus fragments. We assume that the distance from detectable cirrus is a good measure for the likelihood of the presence of undetectable one. Despite the fact that the weak optical signature of thin or diluted cirrus clouds fragments (away from the edges of detectable cirrus) might not be detectable deterministically; they may have a significant optical signature that can be detected in a statistical manner. We show this by analyzing trends in reflectance, aerosol properties and sea surface temperature (SST) for up to 10 km away from detectable cirrus cloud. The presence of undetected cirrus fragments is expected to increase the retrieved AOD and to reduce the inverted SST.

## 2. Data and analysis

This study employs the Level-1 radiance data and Level-2 products (collections 5 and 6) from the MODIS instrument onboard the *Aqua* satellite (Hosoda *et al* 2007, Platnick *et al* 2003, Remer *et al* 2005, Levy *et al* 2013). The data were

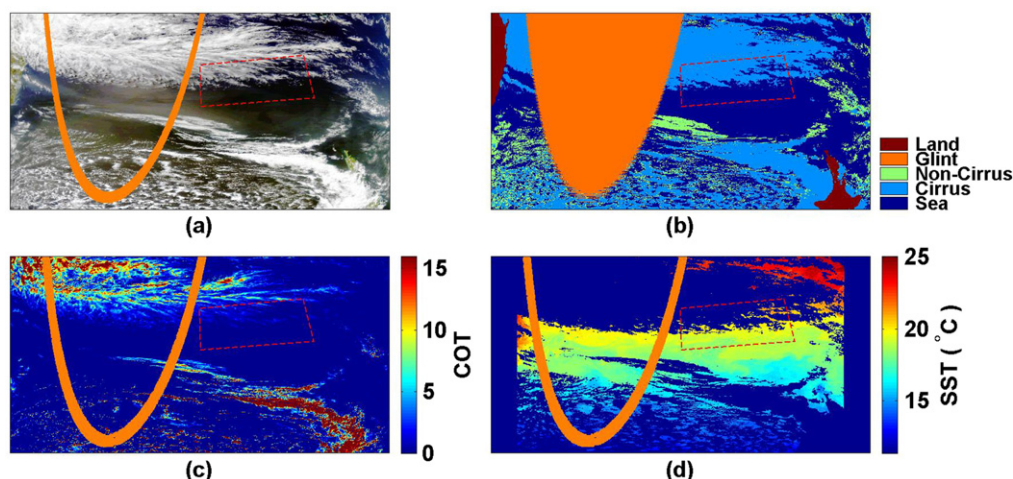


**Figure 1.** Analysis of AQUA-MODIS data from 2 October 2007 at 02:55 GMT over the Pacific Ocean and Australia. (a) Real color image, enhanced to show thin cirrus, (b) feature classification masked image, (c) cloud optical thickness and (d) Level-2 SST. The dashed polygon represents the analyzed area.

selected manually to include the best scenes for examination of cirrus cloud boundaries over the ocean, as free as possible from the presence of other features that might influence the examined trends. We looked for cirrus clouds over the ocean and away from a sun glint, with minimal contribution of shallow clouds below, and with as uniform as possible ocean color. Overall, 23 MODIS data granules were examined from the years 2007–2011 located over the ocean in the mid-latitudes near South America, North America, the West coast of Australia, and Japan.

We utilized the 1 km resolution cloud mask (Ackerman *et al* 1998) along with the (MCF to produce a masked classified image (figure 1(b)) of a selected MODIS granule (figure 1(a)). The classification included cirrus clouds, non-cirrus clouds, land, sun glint and sea surface. We restricted our analysis to areas in which the main cloud type at high altitude is cirrus, thereby avoiding 3D effects arising from proximity to vertically developed clouds (Várnai and Marshak 2002, Marshak *et al* 2006). The average cloud optical thickness over the analyzed areas is  $0.22 \pm 0.41$  (see figure 1(c) and the supporting information). To avoid sun glint, we selected regions (dashed polygon in figure 1) that were at least 30 km away from the edge of the glint zone, as defined by the MODIS mask (Ackerman *et al* 1998). We avoided areas with brighter ocean color (such as sediments near the continents), and the selected areas were at least 30 km away from land features. In addition, the contribution from low clouds forming below the cirrus edges was minimized. Nevertheless, we address the possible effects of analyzing areas with sparse warm clouds in the last section of the results. Euclidean distance from the nearest cirrus cloud was calculated for each cirrus-free pixel within the selected polygons.

Four parameters were analyzed as a function of distance from the nearest cirrus pixels: reflectance, daily and 8-day-average SST (Brown and Minnett 1999), AOD and aerosol Angstrom exponent (Aexp) computed for 553 and 856 nm (Remer *et al* 2005, Levy *et al* 2013). Aexp provides a first

approximation for the suspended particles size. Smaller Aexp values are indication for larger particles (Eck *et al* 1999, Koren *et al* 2007). The analyzed reflectance values were in the visible and near infrared ranges commonly used for cloud and aerosols retrievals (Platnick *et al* 2003, Remer *et al* 2005). They corresponded with bands 1–7 having central wavelengths of 645.5 nm, 856.5 nm, 465.6 nm, 553.6 nm, 1241.6 nm, 1629.1 nm, and 2114.1 nm, respectively. Significant changes in SST are expected to have a much slower rate than 1-day time scale. Hence, in order to minimize the cloud screening of the ocean, where SST cannot be retrieved and to provide a robust SST data, the 8-day average SST is used in addition to the daily SST data. Assuming that the likelihood for a detectable cirrus cloud edge to be located at the same geographical place for several days is low, comparison of a given daily SST with its 8-day average as a function of the distance from the edge of a detectable cirrus cloud can show if there are biases that can be related to the presence of the cirrus there.

Nadir reflectance values acquired from the raw MODIS data product were binned as a function of their distance to the nearest cirrus cloud, and the mean reflectance was calculated for each bin. In a similar manner averages and standard errors of the AOD, Aexp and SST for each bin were calculated. In the MODIS products, in order to increase the signal-to-noise ratio and to have more robust retrievals, the AOD, Aexp and the 8-days SST retrievals are provided on a coarser resolution (compared to the reflectance) using the optical information from a collection of few raw data pixels. In this work, in order to estimate trends in a uniform resolution, we resampled the 8-days SST, AOD and Aexp data into 1 km pixels resolution. In order to avoid any additional assumptions we did not apply any smoothing interpolation on the data. Each 10 km (or 4 km SST) pixel was divided to 1 km pixels, where each of the finer resolution pixels simply inherited the same value as the (coarser resolution) parent pixel.

As a reference to the MODIS cirrus detection-limit, we analyzed the area near the edge of detectable cirrus clouds



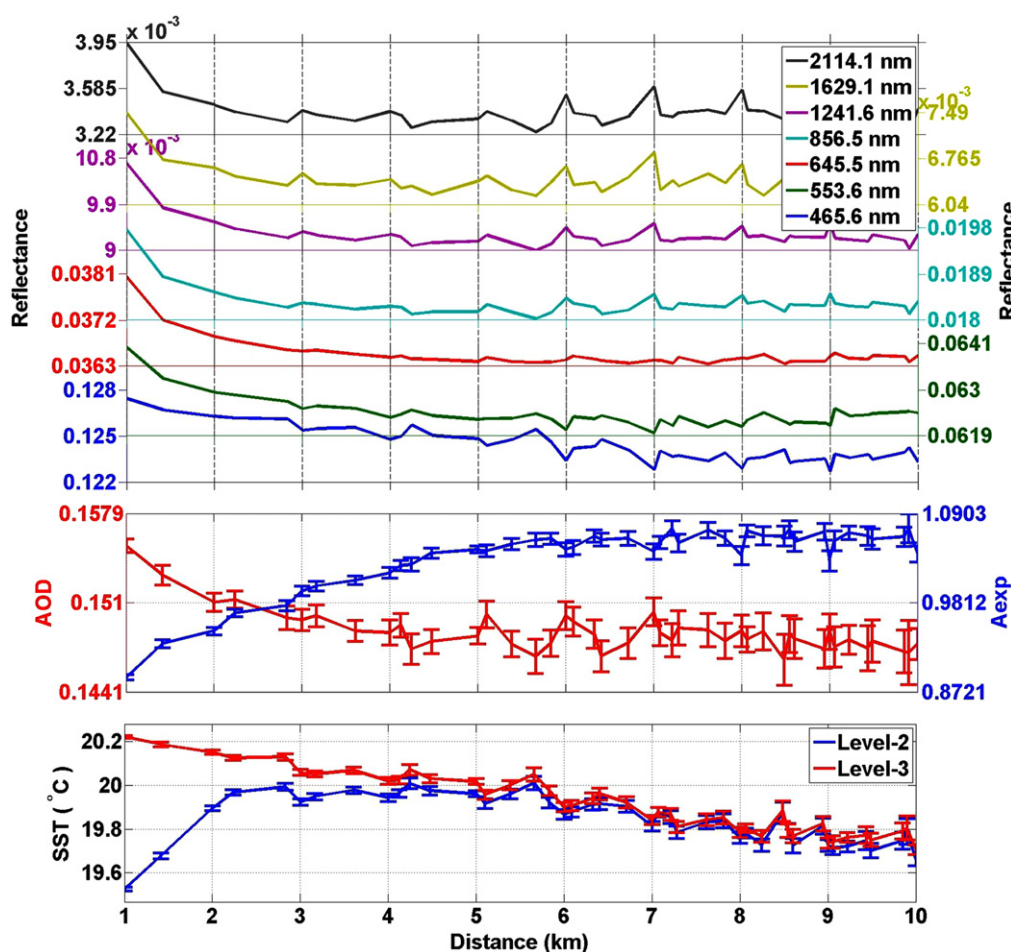


**Figure 2.** Analysis of the reflectance AOD Aexp and SST as a function of the distance from the nearest cloud. (top) Average reflectance values calculated per band plotted as a function of distance from the nearest cirrus pixel. (middle) AOD (red) and Aexp (blue) average values. (bottom) SST average values. The blue line presents the values calculated from the Level-2 daily SST product; the red line presents the Level-3, 8-day-averaged SST product.

using the Level-2 vertical feature mask (VFM) product (Powell *et al* 2010) from the Cloud-Aerosol Lidar with Orthogonal Polarization (CALIOP) aboard CALIPSO. There is an advantage to the LIDAR's much higher sensitivity to weak reflectance signals but on the other hand, its narrow swath footprint ( $\sim 70$  m) provides only a limited view of the atmosphere. As a part of the 'A-Train' satellite constellation (L'Ecuyer and Jiang 2010) the CALIPSO orbit is designed to provide a detailed vertical cross-section of clouds and aerosols over the middle of the AQUA-MODIS swath with  $\sim 1.5$  min time delay.

### 3. Results

Figure 1, shows a MODIS granule over the Pacific Ocean (near Eastern Australia, shown in the upper left corner of the granule) from 2 October 2007. The real color image, features-classification masking, cloud optical depth, and daily SST data of the granule are presented.

The analysis of MODIS bands 1–7 for the same case is shown in figure 2. Average reflectance values (calculated per

band) were plotted as a function of distance from the nearest cirrus pixel. The standard error of the average reflectance values is on the order of 6% (relative); error bars are omitted from the figure for easier visualization. Note the systematic exponential decay of the reflectance as the distance from the nearest cirrus increases. The dependence of the average AOD, Aexp, daily (Level-2) SST, and 8-day average (Level-3) SST on the distance from the nearest cirrus cloud are shown in the lower part of figure 2, with their corresponding standard errors. Note that the average AOD (Aexp) decreases (increases) monotonically with the distance from the nearest cirrus cloud. Changes in the SST are significant only near the cloud showing colder SST for the daily values (Level-2, blue) as compared to the 8-day average, suggesting a contribution of undetected cirrus to the signal.

Similar trends, like the ones presented in figure 2 were observed for all of the analyzed granules (full details can be found in the supporting material). High reflectance values in the solar range of the spectrum suggests possible cirrus contamination near detectable cirrus clouds which, in turn, affects other retrievals over these areas (such as AOD and SST). Assuming that measurements on a distance of 10 km from the

nearest detectable cirrus represent the background conditions, with no significant cirrus contribution, and comparing it to the reflectance values at 1 km away from the detectable cirrus yields systematic changes in the reflectance, AOD, Aexp and most of the SST cases.

The average increase in the AOD and decrease in Aexp is  $0.03 \pm 0.01$  and  $-0.22 \pm 0.20$ , respectively. For each of the 23 cirrus cases studied, the distance at which the cloud-proximity effect on reflectance decays tenfold was calculated for the effect on AOD, Aexp as well as on the raw data reflectance values for each of bands 1–7. The distance for tenfold decay of the effect for AOD is  $5.9 \pm 1.8$  km, for Aexp is  $5.7 \pm 1.9$  km and for the reflectance in the solar bands is  $5.1 \pm 1.9$  km. The trends in the SST as a function of distance from the nearest cirrus were less systematic, but nevertheless in most cases, the daily SST measurements have a clear shift to colder temperatures near the detectable cirrus cloud. When comparing to the 8-day SST data, the average decrease in SST is  $-0.41 \pm 0.55$  °C within 1 km of the cirrus cloud.

To further evaluate the presence of optically thin cirrus clouds that are not detectable by the passive instruments we compared the MODIS cirrus detection with the CALIPSO's backscatter, depolarization and cloud-masking products. To do so we picked daytime CALIPSO data that were acquired close enough to the analyzed MODIS clouds. Figure 3 (upper block) shows an example for such a comparison. The backscatter and depolarization data were collected and averaged vertically along the horizontal levels in which the cirrus was detected (lower left) by the CALIPSO algorithm (Level-2 VFM, Powell *et al* 2010). The averaged backscatter and depolarization lines were plotted (upper right) with the location of the cirrus edge marked according to MODIS (red) and CALIPSO (black). As this is a daytime data the depolarization (upper left) and backscatter data (lower right) are relatively noisy. Nevertheless it can be seen that the edge of the cirrus is characterized by a decay of the backscatter levels to the background levels (where the black line crosses the magenta). It also shows that the MODIS location of the cirrus edge is shifted by  $\sim 15$  km compared to its location in the CALIPSO data. Showing that around the MODIS cirrus edge backscatter values are still slightly elevated indicating a possible residual cloud.

In the nighttime case (figure 3, lower block) the depolarization and backscatter data have a much cleaner signal. The edge of the cirrus cloud (black line on the upper left panel) as determined by the CALIPSO algorithm is located where the backscatter values decay to the cloud-free atmosphere background level. However at the same location the depolarization still shows some residual values suggesting the presence of very weak cirrus cloud beyond the edge of the detectable cirrus (for more examples of day and night CALIPSO data analysis see the supporting material).

Finally, in our analyses we tried to avoid possible contribution of low-level clouds to the observed trends. Nonetheless, formation of low-level clouds below cirrus-flagged areas may occur. Can small, low-level clouds that reside in the analyzed area create similar patterns shown here? To answer this, we conducted a simple theoretical experiment in

which we simulated the cirrus deck scene with gradual contributions from small clouds.

Our tests suggested that the distance-from-the-nearest-cirrus method produces results that are quite immune to the contribution of small clouds (see supporting material for more details). The size and shape differences between the detectable and relatively large, more linear, cirrus deck (used as a proxy for the undetectable cirrus clouds) and the small, mostly circular shallow clouds, allowed for a robust cirrus signal. The distances calculated as a function of the cirrus edge created coherent linear gradients. Local contributions from undetectable (thus small) clouds created circular patterns that might eventually affect the average background properties, but not the trends.

## 4. Discussion

For all of the analyzed cases the reflectance values decreased as a function of the distance from the edge of the detectable cirrus with a similar average tenfold-decay distance of  $5.1 \pm 1.9$  km for all wavelengths. The spectral signature of the increase in the reflectance for the MODIS solar channels is reflected as an increase in AOD and as a reduction in the Angstrom-exponent. The mean increase in AOD at 550 nm is  $0.03 \pm 0.01$  when comparing the AOD values at 1 km away from the edge of the detectable cirrus cloud to the background levels at 10 km. At the same time the Angstrom-exponent decreases when approaching the detectable cloud in  $-0.22 \pm 0.20$ . For both the AOD and Aexp the decay tenfold distance is around 5–6 km. Such systematic enhancement of the optical signal is suggested to be a contribution from the relatively large cirrus particles. Similarly when comparing the daily SST to the 8-day average, the estimated average decrease in the daily SST is  $-0.41 \pm 0.55$  °C within 1 km from the cirrus cloud. Again, suggesting a cooling effect by the undetectable cirrus clouds.

Our findings support the notion of a transition zone near cirrus clouds and represent an initial attempt to quantify the magnitude of that transition zone's effect on the retrieval of other parameters.

While the average range of the effect on the AOD retrieval, found here, is similar to what was found by Kaufman *et al* (2005), here we specify the spatial structure of the effect by using detectable cirrus clouds as markers for the higher likelihood of contribution from undetectable ones. We show the signature of cirrus particles using statistical means over areas in which cirrus clouds cannot be detected by deterministic methods.

The previously defined twilight zone (Koren *et al* 2007) is a complex mix of undetectable cloud fragments, evaporating cloud droplets, humidified aerosols and escaping photons from cloud sides (Wen *et al* 2007). Because cirrus clouds are typically thin and located high in the atmosphere (Sassen and Wang 2008), while aerosol layers are usually located below 5 km height (Winker *et al* 2013), they are usually decoupled. Therefore, this cirrus transition zone is likely to be composed only of thin undetectable cirrus particles.

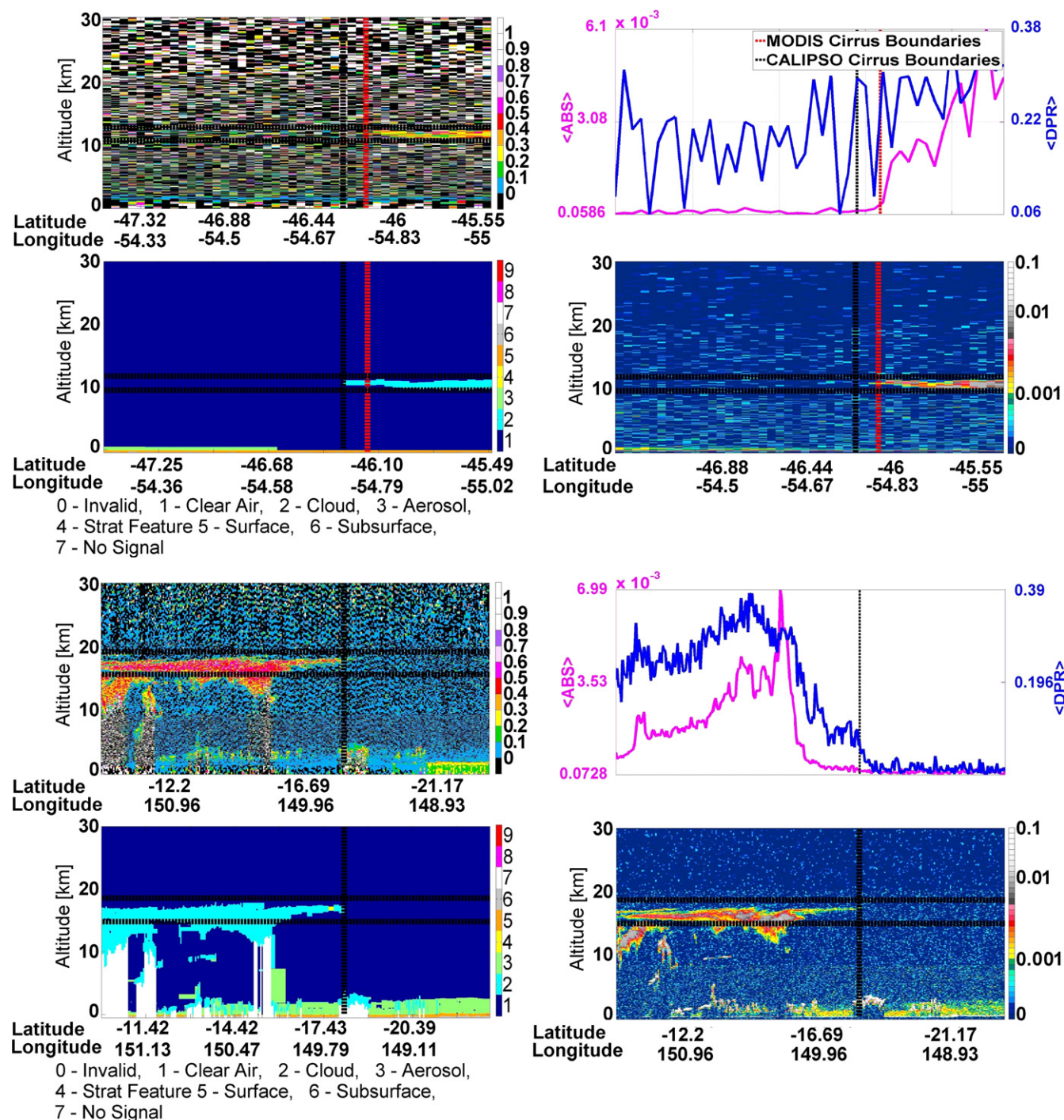


**Figure 3.** Daytime (upper block, 4 panels) data retrieved by CALIPSO on 22 March 2007 over South America and nighttime (lower block) data, 1 January 2012 over Western Pacific ocean. For each block the depolarization ratio is shown on the upper left panel, and the backscatter on the lower right. The bottom left graph presents a vertical feature mask (VFM) and the upper right panel shows the averaged attenuated backscatter ( $\langle \text{ABS} \rangle$ ) at 1064 nm (magenta) and averaged depolarization ( $\langle \text{DPR} \rangle$ ) values (blue) in between the two horizontal dashed black lines shown in the other images. The vertical dashed black line represents the boundary between a cloud feature and clear air from CALIPSO, while the vertical red dashed line represents cirrus boundaries inferred by MODIS. The nighttime case (lower block, 4 panels) of 1 January 2012 over Western Pacific Ocean shows much cleaner depolarization and backscatter signal in which the presence of the thin cirrus can be detected.

Understanding this cirrus transition zone is important both for estimates of cirrus climatology for climate studies, and for understanding how it affects the retrievals of other key climate variables.

## Acknowledgement

This research was funded by the European Research Council under the European Union's Seventh Framework Programme



(FP7/2007–2013)/ERC Grant agreement no. 306965 (CAPRI). The data used in this study were acquired as part of NASA's Earth-Sun System Division and archived and distributed by the MODIS Adaptive Processing System (MODAPS). CALIPSO data were obtained from NASA's Langley Research Center Atmospheric Science Data Center.

## References

- Ackerman S A, Strabala K I, Menzel W P, Frey R A, Moeller C C and Gumley L E 1998 Discriminating clear sky from clouds with MODIS *J. Geophys. Res.* **103** 32141–57
- Baran A J 2012 From the single-scattering properties of ice crystals to climate prediction: a way forward *Atmos. Res.* **112** 45–69
- Barja B and Antuña J C 2011 The effect of optically thin cirrus clouds on solar radiation in Camagüey, Cuba *Atmos. Chem. Phys.* **11** 8625–34
- Bar-Or R Z, Altaratz O and Koren I 2011 Global analysis of cloud field coverage and radiative properties, using morphological methods and MODIS observations *Atmos. Chem. Phys.* **11** 191–200
- Brown O B and Minnett P J 1999 *MODIS Infrared Sea Surface Temperature Algorithm, Version 2.0. MODIS Algorithm Theoretical Basis Document, ATBD-MOD-25* ([http://modis.gsfc.nasa.gov/data/atbd/atbd\\_mod25.pdf](http://modis.gsfc.nasa.gov/data/atbd/atbd_mod25.pdf))
- Charlson R J, Ackerman A S, Bender F A-M, Anderson T L and Liu Z 2007 On the climate forcing consequences of the albedo continuum between cloudy and clear air *Tellus* **59B** 715–27
- Dessler A E and Yang P 2003 The distribution of tropical thin cirrus clouds inferred from terra MODIS data *J. Clim.* **16** 1241–7
- Dupont J C and Haefelin M 2008 Observed instantaneous cirrus radiative effect on surface-level shortwave and longwave irradiances *J. Geophys. Res.* **113** D21202
- Eck T F, Holben B N, Reid J S, Dubovik O, Smirnov A, O'Neill N T, Slutsker I and Kinne S 1999 Wavelength dependence of the optical depth of biomass burning, urban, and desert dust aerosols *J. Geophys. Res.* **104** 31333–49
- Edwards J M, Havemann S, Thelen J C and Baran A J 2007 A new parametrization for the radiative properties of ice crystals: comparison with existing schemes and impact in a GCM *Atmos. Res.* **83** 19–35
- Field P R, Heymsfield A J and Bansemir A 2007 Snow size distribution parameterization for midlatitude and tropical ice clouds *J. Atmos. Sci.* **64** 4346–65
- Field P R, Heymsfield A J, Bansemir A and Twohy C H 2008 Determination of the combined ventilation factor and capacitance for ice crystal aggregates from airborne observations in a tropical anvil cloud *J. Atmos. Sci.* **65** 376–91
- Futyan J M, Russell J E and Harries J E 2005 Determining cloud forcing by cloud type from geostationary satellite data *Geophys. Res. Lett.* **32** L08807
- Gao B C, Kaufman Y J, Tanre D and Li R R 2002b Distinguishing tropospheric aerosols from thin cirrus clouds for improved aerosol retrievals using the ratio of 1.38  $\mu\text{m}$  and 1.24  $\mu\text{m}$  channels *Geophys. Res. Lett.* **29** 1890
- Gao B C, Yang P, Han W, Li R-R and Wiscombe W J 2002a An algorithm using visible and 1.38  $\mu\text{m}$  channels to retrieve cirrus clouds reflectances from aircraft and satellite data *IEEE Trans. Geosci. Remote Sens.* **40** 1659–68
- Heymsfield A J and Miloshevich L M 2003 Parameterizations for the cross-sectional area and extinction of cirrus and stratiform ice cloud particles *J. Atmos. Sci.* **60** 936–56
- Hosoda K, Murakami H, Sakaida F and Kawamura H 2007 Algorithm and validation of sea surface temperature observation using MODIS sensors aboard terra and aqua in the western north pacific *J. Oceanogr.* **63** 267–80
- Huang J, Hsu N C, Tsay S, Jeong M, Holben B N, Berkoff T A and Welton E J 2011 Susceptibility of aerosol optical thickness retrievals to thin cirrus contamination during the BASE-ASIA campaign *J. Geophys. Res.* **116** D08214
- Huang J, Hsu N C, Tsay S-C, Liu Z, Jeong M-J, Hansell R A and Lee J 2013 Use of spaceborne lidar for the evaluation of thin cirrus contamination and screening in the aqua MODIS collection 5 aerosol products *J. Geophys. Res.* **118** 6444–53
- Immler F and Schrems O 2002 LIDAR measurements of cirrus clouds in the northern and southern midlatitudes during INCA (55N, 53S): a comparative study *Geophys. Res. Lett.* **29** 16
- Kahn R A et al 2005 MISR low-light-level calibration, and implications for aerosol retrieval over dark water *J. Atmos. Sci.* **62** 1032–62
- Kaufman Y J et al 2005 A critical examination of the residual cloud contamination and diurnal sampling effects on MODIS estimates of aerosol over ocean *IEEE Trans. Geosci. Remote Sens.* **43** 2886–97
- Khvorostyanov V I and Sassen K 2002 Microphysical processes in cirrus and their impact on radiation *A Mesoscale Modeling Perspective, in Cirrus* ed D Lynch, K Sassen, D O C Starr and G Stephens (Oxford: Oxford University Press) pp 397–432
- King M D, Menzel W P, Kaufman Y J, Tanre D, Gao B-C, Platnick S, Ackerman S A, Remer L A, Pincus R and Hubanks P A 2003 Cloud and aerosol properties, precipitable water, and profiles of temperature and water vapor from MODIS *IEEE Trans. Geosci. Remote Sens.* **41** 442–58
- Koren I, Feingold G, Jiang H L and Altaratz O 2009 Aerosol effects on the inter-cloud region of a small cumulus cloud field *Geophys. Res. Lett.* **36** L14805
- Koren I, Feingold G and Remer L A 2010a The invigoration of deep convective clouds over the Atlantic: aerosol effect, meteorology or retrieval artifact? *Atmos. Chem. Phys.* **10** 8855–72
- Koren I, Remer L A, Altaratz O, Martins J V and Davidi A 2010b Aerosol-induced changes of convective cloud anvils produce strong climate warming *Atmos. Chem. Phys.* **10** 5001–10
- Koren I, Remer L A, Kaufman Y J, Rudich Y and Martins J V 2007 On the twilight zone between clouds and aerosols *Geophys. Res. Lett.* **34** L08805
- L'Ecuyer T and Jiang J 2010 Touring the atmosphere aboard the A-train *Phys. Today* **63** 36–41
- Lee Y K, Yang P, Ackerman S, Huang H-L and Greenwald T J 2010 Global distribution of instantaneous daytime radiative effects of high thin clouds observed by the cloud profiling radar *J. Appl. Remote Sens.* **4** 043543
- Lee Y K, Yang P, Hu Y X, Baum B A, Loeb N G and Gao B C 2006 Potential nighttime contamination of CERES clear-sky fields of view by optically thin cirrus during CRYSTAL-FACE campaign *J. Geophys. Res.* **111** D09203
- Levy R C, Mattoo S, Munchak L A, Remer L A, Sayer A M, Patadia F and Hsu N C 2013 The Collection 6 MODIS aerosol products over land and ocean *Atmos. Meas. Tech.* **6** 2989–3034
- Levy R C, Remer L A, Martins J V, Kaufman Y J, Plana-Fattori A, Redemann J and Wenny B 2005 Evaluation of the MODIS aerosol retrievals over ocean and land during CLAMS *J. Atmos. Sci.* **62** 974–92
- Macke A, Mishchenko M I and Cairns B 1996 The influence of inclusions on light scattering by large ice particles *J. Geophys. Res.* **101** 23311–6
- Marshak A, Platnick S, Varnai T, Wen G Y and Cahalan R F 2006 Impact of three-dimensional radiative effects on satellite retrievals of cloud droplet sizes *J. Geophys. Res.* **111** D09207
- Martins J V, Tanre D, Remer L A, Kaufman Y J, Mattoo S and Levy R 2002 MODIS cloud screening for remote sensing of aerosol over oceans using spatial variability *Geophys. Res. Lett.* **29** 1–4



- Meyer K, Yang P and Gao B-C 2004 Optical thickness of tropical cirrus clouds derived from the MODIS 0.66 and 1.375  $\mu\text{m}$  channels *IEEE Trans. Geosci. Remote Sens.* **42** 833–41
- Platnick S, King M D, Ackerman S A, Paul Menzel W, Baum B A and Frey R A 2003 The MODIS cloud products: algorithms and examples from Terra *IEEE Trans. Geosci. Remote Sens.* **41** 459–73
- Powell K et al 2010 *Cloud-Aerosol LIDAR Infrared Pathfinder Satellite Observations (CALIPSO), Data Management System, Data Products Catalog, Document No: PC-SCI-503, Release 3.2, August 2010* (Hampton, VA, USA: NASA Langley Research Center)
- Remer L A et al 2005 The MODIS aerosol algorithm, products and validation *J. Atmos. Sci.* **62** 947–73
- Roskovensky J K and Liou K N 2003 Detection of thin cirrus using a combination of 1.38  $\mu\text{m}$  reflectance and window brightness temperature difference *J. Geophys. Res.* **108** 4570
- Rossow W and Schiffer R 1999 Advances in understanding clouds from ISCCPP *Bull. Am. Meteorol. Soc.* **80** 2261–87
- Sassen K, Griffin M and Dood G C 1989 Optical scattering and microphysical properties of subvisual cirrus clouds, and climatic implications *J. Appl. Meteorol.* **28** 91–8
- Sassen K and Wang Z 2008 Classifying clouds around the globe with the cloudsat radar: 1-year of results *Geophys. Res. Lett.* **35** 1–5
- Tanré D, Herman M and Kaufman Y J 1996 Information on the aerosol size distribution contained in the solar reflected spectral radiances *J. Geophys. Res.* **101** 19043–60
- Tanré D, Kaufman Y J, Herman M and Mattoo S 1997 Remote sensing of aerosol properties over oceans using the MODIS/EOS spectral radiances *J. Geophys. Res.* **102** 16971–88
- Twohy C H et al 2009 Saharan dust particles nucleate droplets in Eastern Atlantic clouds *Geophys. Res. Lett.* **36** L01807
- Várnai T and Marshak A 2002 Observations of three-dimensional radiative effects that influence MODIS cloud optical thickness retrievals *J. Atmos. Sci.* **59** 1607–18
- Wen G, Marshak A, Cahalan R F, Remer L A and Kleidman R G 2007 3D aerosol-cloud radiative interaction observed in collocated MODIS and ASTER images of cumulus cloud fields *J. Geophys. Res.* **112** D13204
- Winker D M, Tackett J L, Getzewich B J, Liu Z, Vaughan M A and Rogers R R 2013 The global 3D distribution of tropospheric aerosols as characterized by CALIOP *Atmos. Chem. Phys.* **13** 3345–61
- Wylie D, Jackson D, Menzel W and Bates J 2005 Trends in global cloud cover in two decades of HIRS observations *J. Clim.* **18** 3021–31
- Zhang J, Reid J S and Holben B N 2005 An analysis of potential cloud artifacts in MODIS over ocean aerosol optical thickness product *Geophys. Res. Lett.* **32** L15803